Biochemical and Biophysical Research Communications 665 (2023) 169–177

Contents lists available at ScienceDirect

Biochemical and Biophysical Research Communications

journal homepage: www.elsevier.com/locate/ybbrc

FNCaMP, ratiometric green calcium indicator based on mNeonGreen protein

Oksana M. Subach [a], Larisa Varfolomeeva [b], Anna V. Vlaskina [a], Yulia K. Agapova [a], Alena Y. Nikolaeva [a, b], Kiryl D. Piatkevich [c, d, e], Maxim V. Patrushev [a], Konstantin M. Boyko [b], Fedor V. Subach [a, *]

[a] Complex of NBICS Technologies, National Research Center "Kurchatov Institute", Moscow, 123182, Russia
[b] Bach Institute of Biochemistry, Research Centre of Biotechnology of the Russian Academy of Sciences, Moscow, 119071, Russia
[c] School of Life Sciences, Westlake University, Hangzhou, 310024, China
[d] Westlake Laboratory of Life Sciences and Biomedicine, Hangzhou, 310024, China
[e] Institute of Basic Medical Sciences, Westlake Institute for Advanced Study, Hangzhou, 310024, China

ARTICLE INFO

Article history:
Received 18 April 2023
Received in revised form
28 April 2023
Accepted 28 April 2023
Available online 28 April 2023

Keywords:
Genetically encoded calcium indicators
Green fluorescent ratiometric FNCaMP indicator
Calcium imaging
Crystal structure
Chromophore

ABSTRACT

Neurobiologists widely use green genetically encoded calcium indicators (GECIs) for visualization of neuronal activity. Among them, ratiometric GECIs allow imaging of both active and non-active neuronal populations. However, they are not popular, since their properties are inferior to intensiometric GCaMP series of GECIs. The most characterized and developed ratiometric green GECI is FGCaMP7. However, the dynamic range and sensitivity of its large Stock's shift green (LSS-Green) form is significantly lower than its Green form and its molecular design is not optimal. To address these drawbacks, we engineered a ratiometric green calcium indicator, called FNCaMP, which is based on bright mNeonGreen protein and calmodulin from *A. niger* and has optimal NTnC-like design. We compared the properties of the FNCaMP and FGCaMP7 indicators in vitro, in mammalian cells, and in neuronal cultures. Finally, we obtained and analyzed X-ray structure of the FNCaMP indicator.

1. Introduction

Genetically encoded calcium indicators (GECIs) are used in neurobiological studies for visualization of neuronal activity in cultured cells and in vivo in the brain of the model organisms including wide-field calcium imaging and imaging using miniscopes and two-photon microscopes [1,2]. The most numerous GECIs are green fluorescent GECIs, since they have excitation optimal for microscopes [3–5]. The most popular and developed green GECIs are intensiometric with positive calcium response, such as GCaMPs [6–8], GGECOs [9], and NCaMP7 [10]. The molecule of this type of GECIs is composed of one green fluorescent protein (FP) fused to calmodulin-M13-like peptide or troponin C [11]. Despite their popularity related to their great sensitivity and fast dynamics, intensiometric GECIs have drawbacks. Intensiometric GECIs are dim in inactive neurons, when calcium concentration is low, which creates difficulties in identifying labeled neurons and their processes during in vivo imaging and repeated sessions. Artifacts related to out-of-plane motion are noticeable with these GECIs. In addition, it is not possible to quantitatively determine Ca^{2+} concentration using intensiometric GECIs.

Although the ratiometric GECIs can overcome the limitations of intensiometric GECIs, they are less popular and developed. Currently, there are several classes of the ratiometric GECIs based on the molecular design including: the fusion of intensiometric GECIs with complementary FP, Förster Resonance Energy Transfer (FRET) based GECIs, single FP based GECIs, as well as other rarer or uncommon types. Intensiometric GECI can be converted into ratiometric GECI by fusing them to FP characterized by complementary fluorescence emission, such as green-orange

Abbreviations: GECI, Genetically encoded calcium indicator; FP, Fluorescent protein; FRET, Förster Resonance Energy Transfer.

* Corresponding author.
E-mail addresses: subach_om@nrcki.ru (O.M. Subach), l.varfolomeeva@fbras.ru (L. Varfolomeeva), vlaskina_av@nrcki.ru (A.V. Vlaskina), agapova.jk@gmail.com (Y.K. Agapova), nikolaeva_ay@nrcki.ru (A.Y. Nikolaeva), kiryl.piatkevich@westlake.edu.cn (K.D. Piatkevich), patrushev_mv@nrcki.ru (M.V. Patrushev), kmb@inbi.ras.ru (K.M. Boyko), subach_fv@nrcki.ru (F.V. Subach).

https://doi.org/10.1016/j.bbrc.2023.04.108
0006-291X/

MatryoshCaMP6s [12] and green-red GCaMP-R [13]. This type of ratiometric GECIs suffers from the large molecular size and undesired impact of FRET effects, possibly due to overlap between the donor emission and acceptor absorption spectra, converged in one molecule. Tethering an FP to GECIs negatively affects their properties, such as folding efficiency, dynamic range, and calcium affinity [12].

FRET-based ratiometric GECIs use two FPs with highly overlapping emission and absorption spectra in fusion to a calcium-binding domain, such as calmodulin-M13-like peptide or troponin. Cyan-yellow Cameleons [14], green-yellow CaYang, and yellow-red CaYin GECIs [15] or green-red Twitch-GR, Twitch-NR [16], cyan-yellow Twitch-1-5 and cyan-yellow TN-L15, TN-humTnC [17] use calmodulin-M13 like peptide or troponin as calcium-binding domain, respectively. This type of sensors is not popular, since they have a limited dynamic range (up to 60%), lower sensitivity, slower dynamics and requires specilized optical filters for accurate detection of FRET signal. Also FRET-based GECIs have larger size compared to other GEICs, which compliates their delivery to the cells.

Some single FP-based GECIs are inherently ratiometric and consist of single FP fused to calmodulin-M13-like peptide protein. Ratiometric-pericam [18], GEX-GECO1 [9], and FGCaMP7 [19] change their excitation maximum upon calcium ions binding from 390 to 415 to 482–498 nm, preserving the green fluorescence peaked at 506–517 nm. GEM-GECO1 changes its emission maximum from 511 to 455 nm, keeping its excitation maximum at 390–397 nm [9]. The most developed and characterized FGCaMP7 indicator has sensitivity in neurons similar to that for GCaMP6s GECI [19]. Performance of FGCaMP7 was validated in vivo in the mouse and the larval zebrafish brains [19]. In addition to the advantageous ratiometric phenotype, FGCaMP7 has calmodulin-M13-like peptide from *Aspergillus niger* fungus, which prevents its interactions with intracellular space in mammalian cells and allows the generation of the truncated calcium-insensitive version to control for such variations as pH, *etc.* [19]. However, as compared to the anionic form of the FGCaMP7 indicator with excitation at 488 nm, the contrast of the protonated form with excitation at 405 nm was 3-fold smaller in vitro (ΔF/F 9 vs 31), 5.6-fold smaller in HeLa cells, 7-fold smaller in the cultured neurons and 9.6-fold smaller in the brain of zebrafish. In turn, the contrast was undetectable in the mouse brain in vivo under two-photon (2 P) excitation [19]. Also, the topology of the FGCaMP7 sensor was suboptimal in contrast to the NTnC-like design of such GECIs as NCaMP7 [10], YTnC [20], iYTnC2 [21], cNTnC [11] and ncpGCaMP6s [22]. In the NTnC-like desing, the calcium-binding domain is bured inside the FP, allowing the sensor to retain its dynamic range and affinity to Ca^{2+} unchanged, when re-cloned from one plasmid to another. Hence, this type of ratiometric GECIs is the best among other ratiometric GECIs and there is still room for improvement of the single FP-based ratiometric GECIs.

The other types of ratiometric GECIs are less common and include bioluminescent LUCI-GECO1 [22], chemigenetic HaloGFP-Ca1 [23], rHCaMP [24], and dimerization-dependent RA-CaM-B-M13-GA [25]. This type of GECIs are not popular, since they are not optimal for visualization of fast neuronal activity.

In this work, we developed a single FP-based green ratiometric indicator, FNCaMP, which has optimal NTnC-like topology. We tested the performance of the FNCaMP indicator in mammalian cells and neuronal cultures. Finally, we solved and analyzed its crystal structure.

2. Methods

2.1. Cloning of bacterial plasmids, mutagenesis, and library screening

The cloning of bacterial plasmids, mutagenesis, and library screening were performed as described previously [19], using the primers listed in Table S1.

2.2. Protein purification and characterization

Proteins were purified and characterized as described in Ref. [19].

2.3. Isolation of adeno-associated viral particles

rAAV viral particles were prepared as described earlier [19].

2.4. Extraction, cultivation, and transduction of dissociated neuronal cultures

Neuronal cultures were prepared and cultivated as described in [19].

2.5. Protein crystallization

An initial crystallization screening of FNCamp was performed with a robotic crystallization system (Oryx4, Douglas Instr.,UK) and commercially available 96-well crystallization screens (Hampton Research, Aliso Viejo, CA, USA and Anatrace, Maumee, OH, USA) at 15 °C and 4 °C using the sitting drop vapor diffusion method. The protein concentration was 15 mg/mL in the following buffer: 20 mM Tris, 200 mM NaCl, 5 mM Calcium chloride pH 7.5. Optimization of the conditions was performed by the hanging-drop vapor-diffusion method in 24-well VDX plates. Crystals were obtained within 3 days in conditions: 0,1 M MMT buffer pH 8.0,25% PEG 1500.

2.6. Data collection, processing, structure solution, and refinement

The obtained crystals were preliminary characterized using synchrotron source (“Belok” beamline) at NRC Kurchatov Institute (Moscow, Russia). The final FNCaMP diffraction data were collected from a single crystal at 100 K at the beamline ID30A-3 of the ESRF (Grenoble, France). The data were treated using XDS and Aimless programs (Table S2). The structure was solved by the molecular replacement method using MOLREP program and the structure of the NCaMP7 (PDB ID 6XW2) as an initial model. The refinement of the structure was carried out using Refmac5. The visual inspection of electron density maps and the manual rebuilding of the model were carried out using the COOT program. The TLS parameterization was introduced during refinement cycles. In the final model, an asymmetric unit contained one independent copy of the protein of 403 residues, chromophore and 49 water molecules. Eleven *N*-terminal residues as well as the region 298–304 of the loop between calmodulin and M13-like peptide have no electron density.

Visual inspection, comparison, and superposition of the structures were performed as described previously [19].

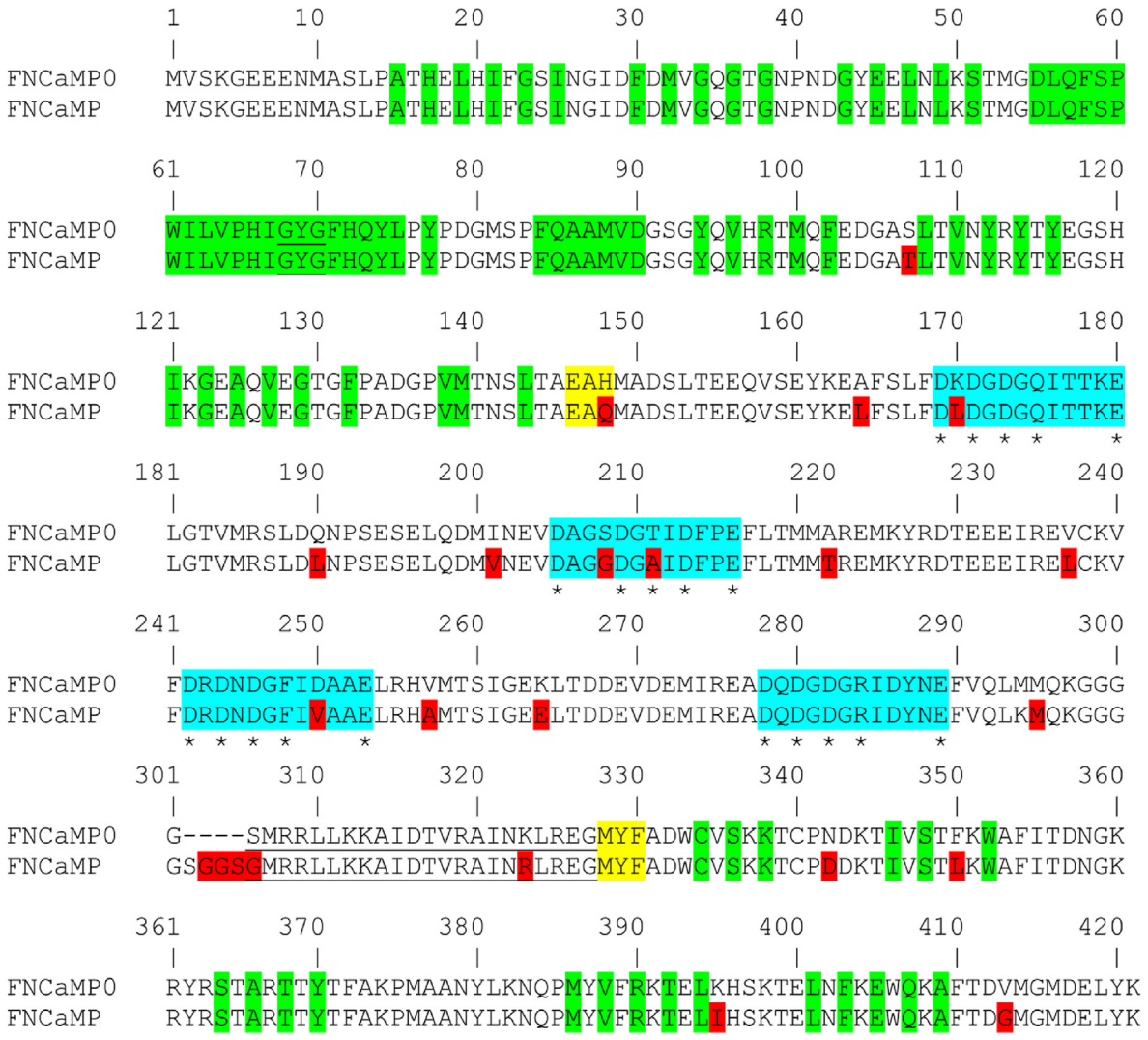

Fig. 1. Alignment of the amino acid sequences for the original FNCaMP0 and FNCaMP indicators. Residues from fluorescent part buried in β-can are highlighted in green. Residues that are forming chromophore and M13-like peptide are underlined. Mutations in FNCaMP related to the original FNCaMP0 are highlighted in red. Linkers between fluorescent and calcium-binding parts are highlighted in yellow. Residues that are forming Ca^{2+}-binding loops are highlighted in cyan. Calcium-coordinating residues are selected with asterisks. (For interpretation of the references to color in this figure legend, the reader is referred to the Web version of this article.)

2.7. Mammalian plasmid construction

Mammalian plasmid construction was performed as described in Ref. [19].

2.8. Mammalian live cell imaging

Confocal imaging of live cells was performed as described in Ref. [19].

2.9. Statistics

To estimate the significance of the difference between two values, we used the Mann–Whitney rank sum test and provided *p* values calculated for the two-tailed hypothesis.

3. Results

3.1. Development of the FNCaMP ratiometric indicator

For the development of the ratiometric green calcium indicator, we inserted CaM-M13 peptide pair (derived from *A. niger*) into the split-version of the mNeonGreen protein and improved its properties using directed molecular evolution in the bacteria. Calcium binding CaM-M13 peptide pair was amplified from the FGCaMP7 indicator [19]. The split-version of the mNeonGreen protein and linkers between calcium-binding domain and the fluorescent domain were amplified from the NCaMP7 indicator [10] (Figs. 1 and 2a). The original FNCaMP0 indicator revealed the ratiometric phenotype, and dissociation constant to calcium ions in the presence of 1 mM Mg^{2+} of 414 ± 32 nM [n = 1.7 ± 0.2], and ΔF/F contrast of 1.6 and 0.4 for Green and LSS-Green forms, respectively.

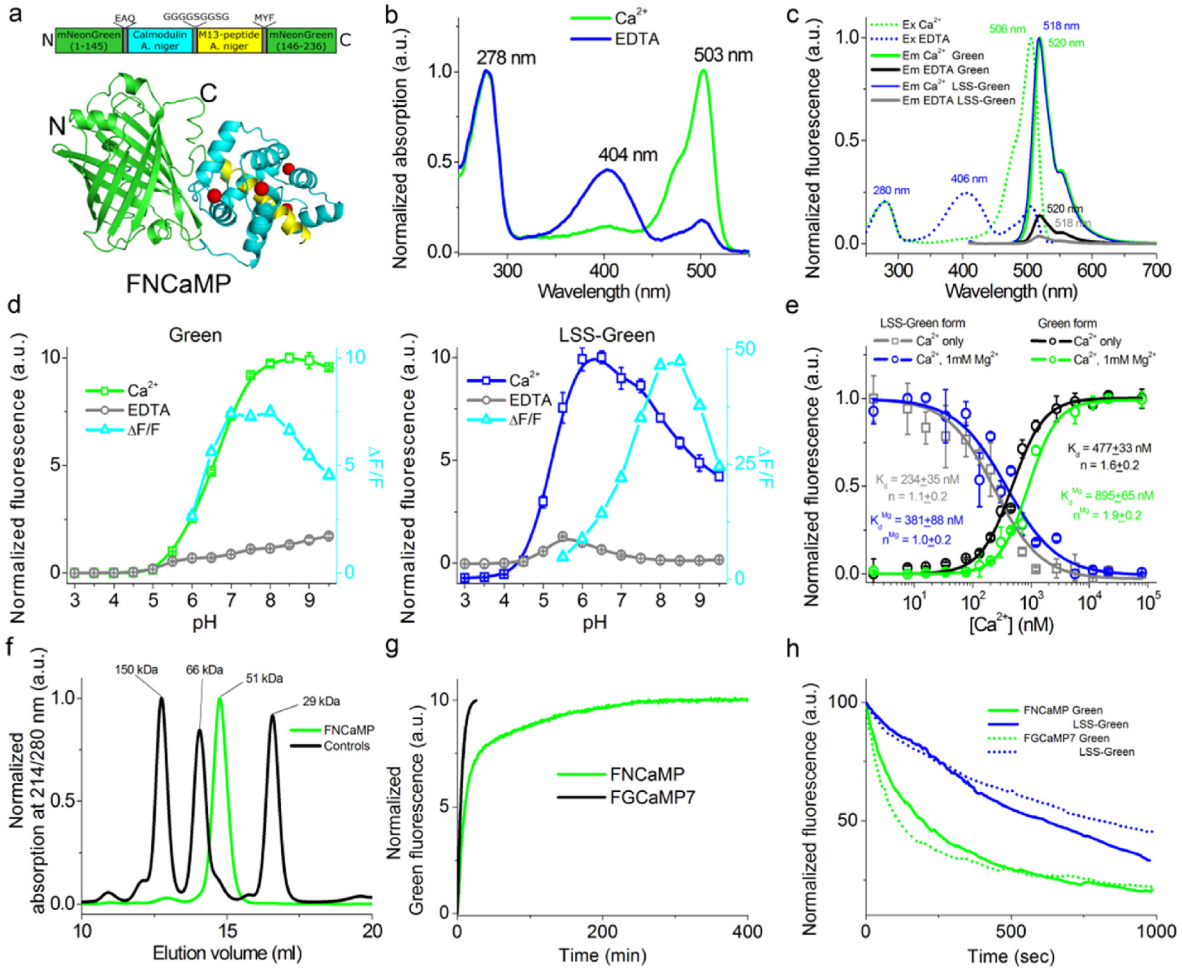

Fig. 2. Structure and in vitro properties of the FNCaMP calcium indicator. (**a**) A schematic representation of the FNCaMP indicator composition and a cartoon representation of its crystal structure (PDB ID— 8OSI). **(b)** Absorption spectra for FNCaMP in Ca^{2+}-bound (5 mM Ca^{2+}) and Ca^{2+}-free (10 mM EDTA) states at pH 7.2. **(c)** Excitation and emission spectra for FNCaMP in Ca^{2+}-bound (5 mM Ca^{2+}) and Ca^{2+}-free (10 mM EDTA) states for Green and LSS-Green forms, pH 7.2. **(d)** Fluorescence intensity for FNCaMP in Ca^{2+}-bound (10 μM Ca^{2+}) and Ca^{2+}-free (10 μM EDTA) states as a function of pH for Green and LSS-Green forms. Error bars represent the standard deviation. **(e)** Ca^{2+} titration curves for Green and LSS-Green forms of FNCaMP in the absence and in the presence of 1 mM $MgCl_2$, pH 7.2. Error bars represent the standard deviation. **(f)** Fast protein liquid chromatography of FNCaMP. FNCaMP (4.5 mg/mL) was eluted in 40 mM Tris-HCl (pH 7.5) and 200 mM NaCl buffer supplemented with 5 mM $CaCl_2$. The experimental molecular weight of FNCaMP (51 kDa) was determined from the dependence of logarithm of control molecular weights vs elution volume (Fig. S2). The theoretical molecular weight of FNCaMP was 48 kDa. (**g**) Maturation curves for the FNCaMP and FGCaMP7 indicators in the presence of 5 mM Ca^{2+}, at 37 °C. (**h**) Photobleaching of FNCaMP and FGCaMP7 in Ca^{2+}-bound (5 mM Ca^{2+}) and Ca^{2+}-free (10 mM EDTA) states at pH 7.2, 45 μM protein concentration. The power of 395/25 nm and 470/40 nm light before objective lens was 0.52 and 1.0 mW/cm^2, respectively. **(d,e,h)** Three (**d,e**) and seven-ten (**h**) replicates were averaged for analysis. (For interpretation of the references to color in this figure legend, the reader is referred to the Web version of this article.)

We subjected FNCaMP0 to several rounds of directed evolution including random mutagenesis followed by a screening on Petri dishes and bacterial lysates. On each round, we imaged bacterial colonies under the Leica fluorescent microscope using LSS-Green (405/40ex and 540/40em) and Green (580/40ex and 535/40em) channels before and after spraying 100 mM EDTA solution. We picked up the colonies exhibiting the largest product of fluorescence contrast in both channels. About 15–20 selected clones were analyzed on bacterial lysates using a plate reader and one clone with the largest fluorescence contrast in both channels was used for the next round of evolution. After eight rounds we found a variant named FNCaMP#28–8, which demonstrated ΔF/F contrasts of 24/25 and dissociation constants to Ca^{2+} in the presence of 1 mM Mg^{2+} of 322 ± 5 nM [n = 3.54 ± 0.15]/303 ± 8 nM [n = 2.78 ± 0.17] for LSS-Green/Green forms, respectively. In HeLa cells, FNCaMP#28–8 reacted to the increase of calcium concentration induced by 2.5 μM ionomycin addition with ΔF/F contrasts of 6.9 ± 4.6 and 11 ± 3 (averaged across 12 cells, two cultures) for LSS-Green and Green forms, respectively. However, then co-expressed in neuronal cultures with the control red *R*-GECO1 indicator, FNCaMP#28-8 had 5.9 ± 0.4 and 4.8 ± 0.9 fold slower decay half times for the Green and LSS-Green forms, respectively, as compared to the dynamics of *R*-GECO1. Slow dynamics of FNCaMP#28-8 mutant prompted us to apply rational mutagenesis to speed up the dynamics of the FNCaMP#28-8 mutant.

First, we increased the length of the linker between CaM and M13-like peptide by four amino acids (GGSG, Fig. 1) according to the linker's length for the NCaMP7 indicator [10]. Next, according to mutations found during the development of the jGCaMP7f indicator [6], we generated FNCaMP#28–8/A164L/V237L double mutant, to replace residues before EF1,2- and EF3,4-hands with bulky side chain ones. The final mutant was named FNCaMP and its dynamics was further characterized in neuronal cultures.

3.2. Characterization of the FNCaMP ratiometric indicator in cultured neurons

Then co-expressed in neurons with the red *R*-GECO1 indicator, FNCaMP demonstrated rise and decay half-times similar to those for *R*-GECO1 (Fig. 3a, c,d and Video S1) and FGCaMP7 [19]. As compared to *R*-GECO1, the ΔF/F response of FNCaMP to calcium transients in neurons was 2.2- and 7.2-fold smaller for Green and LSS-Green forms, respectively (Fig. 3b); the ratiometric ΔR/R response of FNCaMP was 1.4 ± 0.3-fold smaller than ΔF/F response of *R*-GECO1. The ΔF/F responses of the FNCaMP indicator for Green and LSS-Green forms and its ΔR/R response in neurons were 3.2-, 2.5- and 3.1-fold smaller as compared to the same responses for FGCaMP7 [19], respectively. The ΔF/F response for LSS-Green form of FNCaMP was 3.2-fold lower as compared to response of its Green form (Fig. 3b). The difference in ΔF/F responses for two forms of the FNCaMP indicator was 1.3-fold lower as compared to the same difference for the FGCaMP7 indicator [19]. Hence, the FNCaMP can visualize neuronal non-specific activity with similar dynamics, but with 1.4-fold and 3.1-fold lower sensitivity as compared to the *R*-GECO1 and FGCaMP7 indicators, respectively.

3.3. Characterization of the FNCaMP ratiometric indicator in vitro

First, we characterized spectral and biochemical characteristics of the FNCaMP indicator expressed and purified from bacteria. FNCaMP had spectral properties similar to those for FGCaMP7 (Fig. 2b and c and Table 1). The molecular brightnesses of LSS-Green and Green forms of FNCaMP were 1.4-fold smaller and 1.4-fold larger as compared to the brightnesses of the respective forms of the FGCaMP7 indicator, respectively (Table 1).

The addition of 1 mM Mg^{2+} ions (conditions resembling those inside the cytosol of mammalian cells) decreased the ΔF/F dynamic range of LSS-Green form of FNCaMP by 2.8-fold (Table 1); this Mg^{2+}-dependence was not observed for the FGCaMP7 indicator. In the presence of 1 mM Mg^{2+} ions, the dynamic ranges of LSS-Green and Green forms of FNCaMP were similar or 3.6-fold smaller as compared to the same forms of FGCaMP7, respectively (Table 1).

The shapes of pH dependences for FNCaMP and FGCaMP7 indicators were different, but the dynamic range of both indicators was sensitive to variations of pH (Fig. 2d and Table 1).

The affinities to Ca^{2+} in the presence of Mg^{2+} ions for LSS-Green and Green forms of FNCaMP were 1.7- and 3.7-fold lower as compared to FGCaMP7, respectively (Fig. 2e and Table 1). The calcium affinity in the presence of Mg^{2+} ions for Green form of FNCaMP was 2.3-fold lower than the calcium affinity for LSS-Green form (Table 1); the calcium affinities for both forms of the FGCaMP7 indicator were practically the same. Similarly to FGCaMP7, the addition of 1 mM Mg^{2+} ions decreased the calcium affinity of both Green and LSS-Green forms in 1.9- and 1.6-fold, respectively (Fig. 2e and Table 1).

FNCaMP eluted on fast protein liquid chromatography as a monomer (Fig. 2f) similar to FGCaMP7 [19].

FNCaMP matured till 50% at 37 °C for 11 min (Fig. 2g and Table 1). This time was 2.8-fold slower as compared to the FGCaMP7 indicator.

The photostabilities of LSS-Green and Green forms of FNCaMP under metal halide lamp illumination were 1.3-fold lower and 1.8-fold higher as compared to FGCaMP7 (Fig. 2h and Table 1).

Hence, FNCaMP was superior to the FGCaMP7 indicator in increased brightness and photostability of Green form, but inferior to it in decreased brightness and photostability of LSS-Green form,

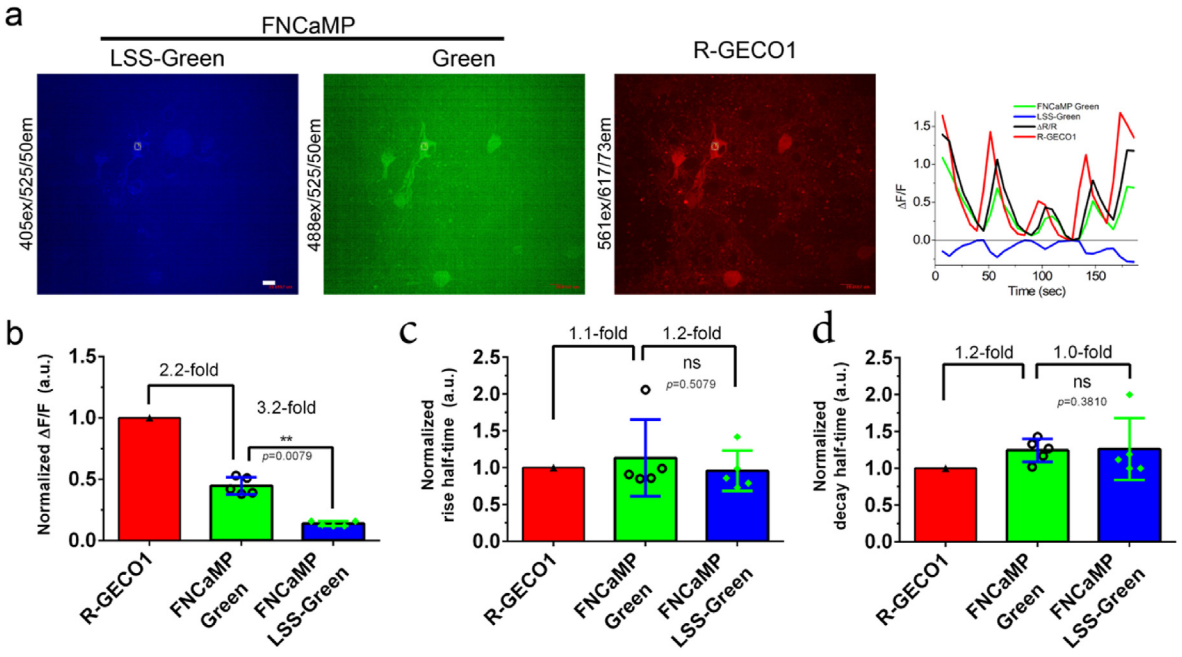

Fig. 3. Comparison of the performance of the FNCaMP indicator with control *R*-GECO1 red indicator in cultured neurons during their non-specific activity. Neuronal cultures were transduced on day in vitro 4th with a mixture of rAAVs carrying the nuclear export signals (NES)- *R*-GECO1 and NES-FNCaMP. (**a**) Confocal images of neurons co-expressing ratiometric indicator FNCaMP at 405 nm and 488 nm excitations and red indicator *R*-GECO1 at 561 nm excitation were acquired on DIV 14,15th. Example of ΔF/F traces for the one selected cell labeled with circle. Scale bar: 20 μm. (**b-d**) Average ΔF/F responses (**b**), rise (**c**), and decay (**d**) halftimes for the FNCaMP indicator normalized to the same parameters for the *R*-GECO1. (**b**–**d**) Error bars are the standard deviations across five cells. Ns, not significant; p, the level of statistical significance; **, p-value is 0.001–0.01. (For interpretation of the references to color in this figure legend, the reader is referred to the Web version of this article.)

Table 1
In vitro properties of the purified FNCaMP indicator compared to FGCaMP7.[a] mEGFP (quantum yield, QY = 0.60 ref. [27]) and mTagBFP2 (QY = 0.64 ref. [28]) were used as reference standards for Green and LSS-Green states, respectively.[b] Extinction coefficient was determined by alkaline denaturation. C Brightness was normalized to mEGFP, with a QY of 0.60 and an extinction coefficient of 53.3 ± 3.6 mM−1cm−1. d p*Ka* values were calculated according to the pH dependence of fluorescence.[e] Experimental data were fitted to Hill equation. Hill coefficients are shown in brackets. K_d values for GCaMP6s in the absence and in the presence of 1 mM $MgCl_2$ were 144 ± 9 nM (4.0 ± 0.6) and 217 ± 16 nM (4.0 ± 0.6), respectively.[f] mEGFP had a maturation half-time of 13 min[g] The power of 395/25 nm and 470/40 nm light before objective lens was 0.52 and 1.0 mW/cm^2, respectively. ND, not determined. * The values for FGCaMP7 were from Ref. [19] except data marked with asterisk, which were measured in parallel.

Properties		Proteins			
		FNCaMP		FGCaMP7	
		Apo	Sat	Apo	Sat
Absorption/Excitation maximum (nm)		403/406	503/506	400/403 *	498/501 *
Emission maximum (nm)		518	520	516	
Quantum yield[a]		0.29 ± 0.10	0.62 ± 0.10	0.35 ± 0.01 *	0.62 ± 0.01 *
ε (mM-1cm-1) b		53 ± 11	140 ± 12	60 ± 4 *	101 ± 12 *
Brightness vs mEGFP (%)[c]		48	271	66 *	196 *
ΔF/F	LSS-Green	27 ± 6		8.3 ± 0.3	
	Green	7.3 ± 0.9		37.4 ± 0.9	
ΔF/F with 1 mM $MgCl_2$	LSS-Green	9.5 ± 0.5		9.1 ± 1.0	
	Green	8.7 ± 0.8		31.7 ± 1.5	
pK_a (LSS-Green)[d]		5.23 ± 0.05; 8.93 ± 0.13	5.04 ± 0.01; 6.52 ± 0.04	6.63 ± 0.20	6.00 ± 0.20
pK_a (Green)[d]		6.98 ± 0.05	6.56 ± 0.01	5.28 ± 0.10; 7.81 ± 0.10	6.87 ± 0.01
K_d (nM)[e]	LSS-Green	234 ± 35 (n = 1.1 ± 0.2)		130 ± 10 (n = 2.7 ± 0.1)	
	Green	477 ± 33 (n = 1.6 ± 0.2)		160 ± 10 (n = 2.6 ± 0.2)	
K_d (nM) with 1 mM $MgCl_2$[s]	LSS-Green	381 ± 88 (n = 1.0 ± 0.2)		230 ± 5 (n = 2.2 ± 0.1)	
	Green	895 ± 65 (n = 1.9 ± 0.2)		240 ± 6 (n = 2.3 ± 0.2)	
Protein state		Monomer		monomer	
Maturation half-time (min)[f]		ND	11	ND	4 *
Photobleaching half-time (sec)[g]		616 ± 207	195 ± 73	795 ± 360 *	110 ± 26 *

decreased dynamic range of Green form, and lower calcium affinities of both forms.

3.4. Characterization of the FNCaMP ratiometric indicator in HeLa cells

In HeLa mammalian cells FNCaMP responded to ionomycin-induced elevations of calcium ions concentration with ΔF/F values of 5.4 ± 2.2 and 5.2 ± 1.2 for LSS-Green and Green forms, respectively (Fig. 4), and ΔR/R values of 41 ± 21. *R*-GECO1 co-expressed in the same cells showed ΔF/F response value of 6.2 ± 2.0. The ΔF/F responses of the LSS-Green and Green forms of FGCaMP7 were the same or 2-fold larger than the responses of the respective forms of the FNCaMP indicator (Fig. 4c). The responses of both forms of FNCaMP were the same, in contrast to FGCaMP7, whose Green form had a response 2.2-fold larger than that for LSS-Green form (Fig. 4c). Hence, in the cytosol of mammalian cells, FNCaMP had a similar or 2.2-fold lower response to Ca^{2+} transients as compared to the *R*-GECO1 and FGCaMP7 indicators, respectively.

3.5. Crystal structure of the FNCaMP indicator

To understand the molecular basis of FNCaMP's fluorescence sensitivity to Ca^{2+}, we solved the crystal structure of FNCaMP in the presence of Ca^{2+} at 2.42 Å resolution. FNCaMP has a monomeric state in the crystal, supporting the biochemical data. The ^{68}GYG^{70} chromophore is in *cis* configuration and forms five direct and three water-mediated hydrogen bonds (H-bonds) with the neighboring residues (Fig. 5a). The contacts of the OH group of the chromophore's tyrosine with surrounding amino acids in the FNCaMP indicator are different from those in the NCaMP7 indicator, while both indicators are based on mNeonGreen protein. The phenolic OH-group in the chromophore of the FNCaMP indicator forms one direct H-bond with the SH-group of C334 and three water-mediated bonds with the OH-group of S335, carbonyl groups of C334 as well as NH-group of R389 (Fig. 5b). In opposite, in NCaMP7 it forms only three water-mediated interactions with other amino acids. Since A164L and V237L substitutions in −5 positions before the consensus motifs in calcium-binding EF-hands 1 and 3 in FNCaMP0 caused about 5-fold acceleration of decay half-times in neurons, we analyzed the surroundings of these substitutions (Fig. 5c and d). Both L164 and V237 are located in the hydrophobic pockets in the interface between M13-peptide and calmodulin in the regions of the 1, 2, and 3 consensus calcium-binding motifs.

4. Discussion

Based on mNeonGreen protein and calmodulin from *A. niger*, we created a ratiometric green calcium indicator, FNCaMP, and characterized its properties in vitro, in mammalian cells, in neuronal culture, and analyzed its crystal structure.

By many parameters, FNCaMP is inferior to FGCaMP7 including lower contrast of Green form, lower affinity to Ca^{2+} and as a consequence lower sensitivity in neuronal cultures. However, FNCaMP has an advantageous NTnC-like design with the insertion of calmodulin inside the FP, which ensures that *N*- and *C*-terminus are remote from the calcium-binding domain of the sensor. Similarly to FGCaMP7, calmodulin from fungus used in the FNCaMP indicator ensures its inertness to the cytosolic environment of the mammalian cells. Overall, the FNCaMP indicator could be further improved, but still can be used for calcium imaging in mammalian cells and neurons and provides an alternative platform for the development of the ratiometric calcium indicator.

Using the crystal structure of FNCaMP, we explained the molecular basis of FNCaMP's function. We suggested that FNCaMP's fluorescence sensitivity to Ca^{2+} may be provided by the interaction of OH-group of Y227 from calmodulin with the phenolic OH-group of the chromophore via H-bonds with C334 SH-group and K351 carbonyl group (Fig. 5a and b). The fluorescence sensitivity to calcium ions in NCaMP7 [10] and GCaMP6m [26] was attributed to similar interaction of the OH-group of the chromophore in the fluorescent domain and corresponding Y225 and Y380 in the

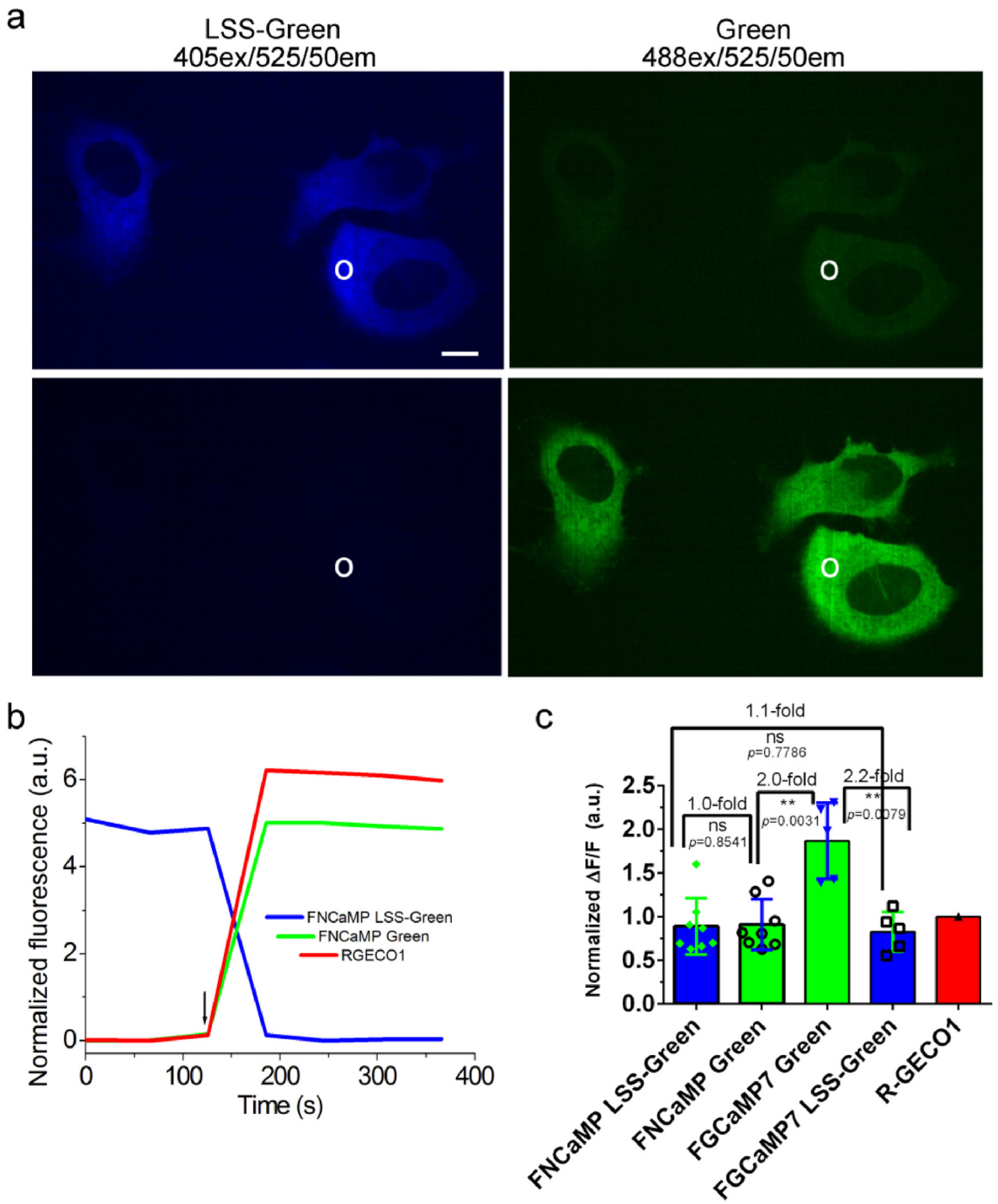

Fig. 4. The response of the FNCaMP indicator to calcium transients in HeLa cells. (**a**) Confocal images of HeLa cells co-expressing green FNCaMP and red *R*-GECO1 (not shown) indicators in LSS-Green and Green channels before (upper panels) and after 2.5 μM ionomycin addition (lower panels). (**b**) The graph illustrate changes in fluorescence of FNCaMP and co-expressed *R*-GECO1 GECI in response to 2.5 μM ionomycin in the area indicated with white circle. Ionomycin addition is shown with arrow. Scale bar: 10 μm. (**c**) Normalized ΔF/F responses averaged across 5–8 cells and 3–4 cultures. Ns, not significant; p, the level of statistical significance; **, p-value is 0.001–0.01. (For interpretation of the references to color in this figure legend, the reader is referred to the Web version of this article.)

calcium-binding domain. We also suggest that the ratiometric phenotype of FNCaMP, which consists in the protonation-deprotonation of the OH-group of the tyrosine chromophore, is probably provided with a hydrogen bond network between the OH-group of the chromophore and hydroxyl-group of S336 and further to water molecules and other residues of the FNCaMP indicator.

The crystal structure of FNCaMP allowed to explain why changing the amino acids at the −5 positions before the consensus motifs in calcium-binding EF-hands 1 and 3 in FNCaMP0 led to faster kinetics in neurons for the FNCaMP indicator compared to FNCaMP0 (Fig. 5c and d). The fluorescence response rate of the calcium indicator depends on the association-dissociation rate between calmodulin and M13-peptide [8]. The A317L mutation in

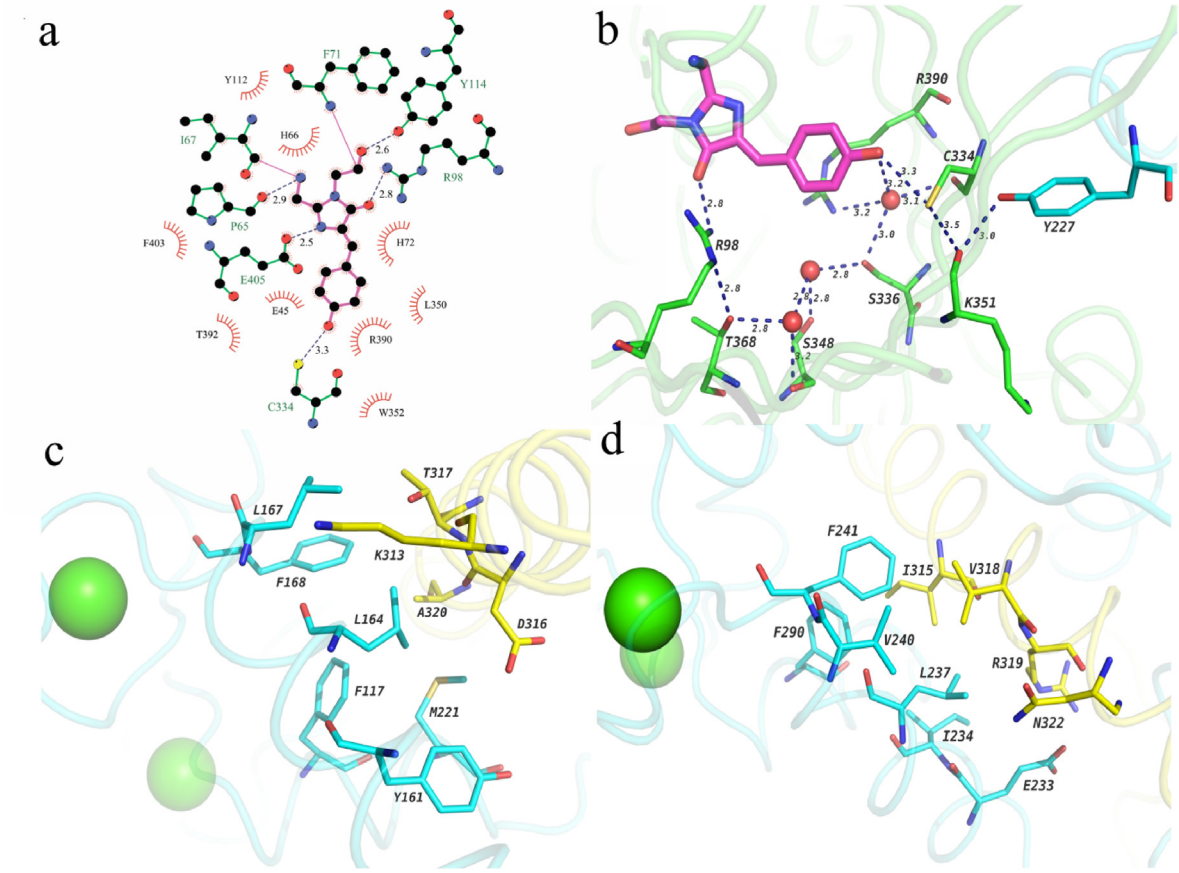

Fig. 5. Crystal structure of the FNCaMP indicator. (a) Chromophore environment in the FnCaMP structure prepared with Ligplot [29]. (b) The hydrogen bond network (dashed blue lines), formed between OH-group of the chromophore, neigbouring amino acids and solvent molecules. (c,d) The environment of L169 (c) and L242 (d) residues within 8 Å. Residues of the mNeonGreen, CaM, M13-peptide, and chromophore are colored in green, blue, yellow, and magenta, respectively. Solvent molecules and Ca^{2+} are shown as red and green spheres, respectively. (For interpretation of the references to color in this figure legend, the reader is referred to the Web version of this article.)

the calmodulin/M13-peptide interface of jGCaMP7f resulted in faster flurescence respose to Ca^{2+} ions [8]. Thus, we can assume that leucine substitutions (L164 and L237) positioned in the same interface of FNCaMP cause the faster kinetics of the sensor.

Accession numbers

The coordinates and structure factor files of the FNCaMP indicator was deposited into protein data bank (www.rcsb.org) with the accession number PDB ID 8OSI.

Institutional review board statement

The animal study protocol was approved by the Institutional Ethics Committee of the National Research Center "Kurchatov Institute" (NG-1/109 PR of February 13, 2020) and was performed in accordance with the Russian Federation Order Requirements N 267 M3 and the National Institutes of Health Guide for the Care and Use of Laboratory Animals.

Declaration of competing interest

The authors declare that they have no known competing financial interests or personal relationships that could have appeared to influence the work reported in this paper.

Acknowledgments

This research was partially funded by grant of the National Research Center Kurchatov Institute (developing the FNCaMP); by the Russian Science Foundation grant No 21-74-20135 to K.M.B. (crystallization, data collection and structural studies); by the Ministry of Science and Higher Education of the Russian Federation for the development of the Kurchatov Center for Genome Research 075-15-2019-1659 to M.V.P. (protein purification), by start-up funding from the Foundation of Westlake University, Westlake Laboratory of Life Sciences and Biomedicine, National Natural Science Foundation of China grants 32050410298 and 32171093; and by a 2020 BBRF Young Investigator Grant 28961 to K.D.P (characterization of FNCaMP in mammalian cells). The work was also supported by the Resource Centers department of the National Research Center Kurchatov Institute (imaging of bacteria and cultivation of neuronal cultures).

Appendix A. Supplementary data

Supplementary data to this article can be found online at https://doi.org/10.1016/j.bbrc.2023.04.108.

References

[1] A.K. Nietz, L.S. Popa, M.L. Streng, R.E. Carter, S.B. Kodandaramaiah, T.J. Ebner, Wide-field calcium imaging of neuronal network dynamics in vivo, Biology 11 (2022).

[2] J. Day-Cooney, R. Dalangin, H. Zhong, T. Mao, Genetically encoded fluorescent sensors for imaging neuronal dynamics in vivo, J. Neurochem. 164 (2023) 284–308.
[3] Kiryl D. Piatkevich, Mitchell H. Murdock, F.V. Subach, Advances in engineering and application of optogenetic indicators for neuroscience, Appl. Sci. 9 (2019).
[4] M. Wang, Y. Da, Y. Tian, Fluorescent proteins and genetically encoded biosensors, Chem. Soc. Rev. 52 (2023) 1189–1214.
[5] S.Y. Wu, Y. Shen, I. Shkolnikov, R.E. Campbell, Fluorescent indicators for biological imaging of monatomic ions, Front. Cell Dev. Biol. 10 (2022), 885440.
[6] H. Dana, Y. Sun, B. Mohar, B.K. Hulse, A.M. Kerlin, J.P. Hasseman, G. Tsegaye, A. Tsang, A. Wong, R. Patel, J.J. Macklin, Y. Chen, A. Konnerth, V. Jayaraman, L.L. Looger, E.R. Schreiter, K. Svoboda, D.S. Kim, High-performance calcium sensors for imaging activity in neuronal populations and microcompartments, Nat. Methods 16 (2019) 649–657.
[7] T.W. Chen, T.J. Wardill, Y. Sun, S.R. Pulver, S.L. Renninger, A. Baohan, E.R. Schreiter, R.A. Kerr, M.B. Orger, V. Jayaraman, L.L. Looger, K. Svoboda, D.S. Kim, Ultrasensitive fluorescent proteins for imaging neuronal activity, Nature 499 (2013) 295–300.
[8] Y. Zhang, M. Rozsa, Y. Liang, D. Bushey, Z. Wei, J. Zheng, D. Reep, G.J. Broussard, A. Tsang, G. Tsegaye, S. Narayan, C.J. Obara, J.X. Lim, R. Patel, R. Zhang, M.B. Ahrens, G.C. Turner, S.S. Wang, W.L. Korff, E.R. Schreiter, K. Svoboda, J.P. Hasseman, I. Kolb, L.L. Looger, Fast and sensitive GCaMP calcium indicators for imaging neural populations, Nature 615 (2023) 884–891.
[9] Y. Zhao, S. Araki, J. Wu, T. Teramoto, Y.F. Chang, M. Nakano, A.S. Abdelfattah, M. Fujiwara, T. Ishihara, T. Nagai, R.E. Campbell, An expanded palette of genetically encoded Ca(2) indicators, Science 333 (2011) 1888–1891.
[10] O.M. Subach, V.P. Sotskov, V.V. Plusnin, A.M. Gruzdeva, N.V. Barykina, O.I. Ivashkina, K.V. Anokhin, A.Y. Nikolaeva, D.A. Korzhenevskiy, A.V. Vlaskina, V.A. Lazarenko, K.M. Boyko, T.V. Rakitina, A.M. Varizhuk, G.E. Pozmogova, O.V. Podgorny, K.D. Piatkevich, E.S. Boyden, F.V. Subach, Novel genetically encoded bright positive calcium indicator NCaMP7 based on the mNeonGreen fluorescent protein, Int. J. Mol. Sci. 21 (2020).
[11] Oksana M. Subach, Anna V. Vlaskina, Yuliya K. Agapova, Dmitriy A. Korzhenevskiy, Alena Y. Nikolaeva, Anna M. Varizhuk, Maksim F. Subach, Maxim V. Patrushev, Kiryl D. Piatkevich, M. Konstantin, F.V. Boyko, Subach, cNTnC and fYTnC2, genetically encoded green calcium indicators, Based on Troponin C from Fast Animals 23 (2022), 14614.
[12] C. Ast, J. Foret, L.M. Oltrogge, R. De Michele, T.J. Kleist, C.H. Ho, W.B. Frommer, Ratiometric Matryoshka biosensors from a nested cassette of green- and orange-emitting fluorescent proteins, Nat. Commun. 8 (2017) 431.
[13] J.H. Cho, C.J. Swanson, J. Chen, A. Li, L.G. Lippert, S.E. Boye, K. Rose, S. Sivaramakrishnan, C.M. Chuong, R.H. Chow, The GCaMP-R family of genetically encoded ratiometric calcium indicators, ACS Chem. Biol. 12 (2017) 1066–1074.
[14] A. Miyawaki, O. Griesbeck, R. Heim, R.Y. Tsien, Dynamic and quantitative Ca2+ measurements using improved cameleons, Proc. Natl. Acad. Sci. U.S.A. 96 (1999) 2135–2140.
[15] Y. Ding, H.W. Ai, H. Hoi, R.E. Campbell, Forster resonance energy transfer-based biosensors for multiparameter ratiometric imaging of Ca2+ dynamics and caspase-3 activity in single cells, Anal. Chem. 83 (2011) 9687–9693.
[16] D. Zhang, E. Redington, Y. Gong, Rational engineering of ratiometric calcium sensors with bright green and red fluorescent proteins, Commun.Biol. 4 (2021) 924.
[17] N. Heim, O. Griesbeck, Genetically encoded indicators of cellular calcium dynamics based on troponin C and green fluorescent protein, J. Biol. Chem. 279 (2004) 14280–14286.
[18] T. Nagai, A. Sawano, E.S. Park, A. Miyawaki, Circularly permuted green fluorescent proteins engineered to sense Ca2+, Proc. Natl. Acad. Sci. U.S.A. 98 (2001) 3197–3202.
[19] N.V. Barykina, V.P. Sotskov, A.M. Gruzdeva, Y.K. Wu, R. Portugues, O.M. Subach, E.S. Chefanova, V.V. Plusnin, O.I. Ivashkina, K.V. Anokhin, A.V. Vlaskina, D.A. Korzhenevskiy, A.Y. Nikolaeva, K.M. Boyko, T.V. Rakitina, A.M. Varizhuk, G.E. Pozmogova, F.V. Subach, FGCaMP7, an improved version of fungi-based ratiometric calcium indicator for in vivo visualization of neuronal activity, Int. J. Mol. Sci. 21 (2020).
[20] N.V. Barykina, D.A. Doronin, O.M. Subach, V.P. Sotskov, V.V. Plusnin, O.A. Ivleva, A.M. Gruzdeva, T.A. Kunitsyna, O.I. Ivashkina, A.A. Lazutkin, A.Y. Malyshev, I.V. Smirnov, A.M. Varizhuk, G.E. Pozmogova, K.D. Piatkevich, K.V. Anokhin, G. Enikolopov, F.V. Subach, NTnC-like genetically encoded calcium indicator with a positive and enhanced response and fast kinetics, Sci. Rep. 8 (2018), 15233.
[21] D.A. Doronin, N.V. Barykina, O.M. Subach, V.P. Sotskov, V.V. Plusnin, O.A. Ivleva, E.A. Isaakova, A.M. Varizhuk, G.E. Pozmogova, A.Y. Malyshev, I.V. Smirnov, K.D. Piatkevich, K.V. Anokhin, G.N. Enikolopov, F.V. Subach, Genetically encoded calcium indicator with NTnC-like design and enhanced fluorescence contrast and kinetics, BMC Biotechnol. 18 (2018) 10.
[22] Y. Qian, V. Rancic, J. Wu, K. Ballanyi, R.E. Campbell, A bioluminescent Ca(2+) indicator based on a topological variant of GCaMP6s, Chembiochem : Eur. J.Chem. Biol. (2018).
[23] W. Zhu, S. Takeuchi, S. Imai, T. Terada, T. Ueda, Y. Nasu, T. Terai, R.E. Campbell, Chemigenetic indicators based on synthetic chelators and green fluorescent protein, Nat. Chem. Biol. 19 (2023) 38–44.
[24] L. Wang, J. Hiblot, C. Popp, L. Xue, K. Johnsson, Environmentally sensitive color-shifting fluorophores for bioimaging, Angew. Chem. 59 (2020) 21880–21884.
[25] Y. Ding, J. Li, J.R. Enterina, Y. Shen, I. Zhang, P.H. Tewson, G.C. Mo, J. Zhang, A.M. Quinn, T.E. Hughes, D. Maysinger, S.C. Alford, Y. Zhang, R.E. Campbell, Ratiometric biosensors based on dimerization-dependent fluorescent protein exchange, Nat. Methods 12 (2015) 195–198.
[26] J. Ding, A.F. Luo, L. Hu, D. Wang, F. Shao, Structural Basis of the Ultrasensitive Calcium Indicator GCaMP6, Science China, Life sciences, 2014.
[27] R.Y. Tsien, The green fluorescent protein, Annu. Rev. Biochem. 67 (1998) 509–544.
[28] O.M. Subach, P.J. Cranfill, M.W. Davidson, V.V. Verkhusha, An enhanced monomeric blue fluorescent protein with the high chemical stability of the chromophore, PLoS One 6 (2011), e28674.
[29] A.C. Wallace, R.A. Laskowski, J.M. Thornton, LIGPLOT: a program to generate schematic diagrams of protein-ligand interactions, Protein Eng. 8 (1995) 127–134.